Fabrication of plasmonic crystals using programmable nanoreplica molding process

Longju Liu[a], Mohsin A. Badshah[b], Seok-min Kim[b], and Meng Lu*[ac]

[a]Dept. of Electrical and Computer Engineering, Iowa State Univ., Ames, IA, USA 50011; [b]School of Mechanical Engineering, Chung-Ang Univ., Seoul 156-756 Republic of Korea; [c]Dept. of Mechanical Engineering, Iowa State Univ., Ames, IA USA 50011;

ABSTRACT

The development of many photonic devices, such as photonic integrated circuit, optical sensors, and photovoltaic devices, demands low-cost and reliable fabrication technologies to fabricate sub-wavelength features. Here, we report a programmable nanoreplica molding process, which is capable of producing photonic devices with a variety of sub-micrometer patterns. The process utilizes a stretchable plastic mold to generate the desired periodic pattern using a UV-curable polymer on plastic substrates. During the replica molding process, a uniaxial force is applied to the mold and results in changes of the periodic structure, which locates on the surface of the mold. The geometry of the replicated pattern, including the lattice constant and arrangement, is determined by the magnitude and direction of the force. As an example, we present a plasmonic crystal device with surface plasmon resonances carefully tuned by using the uniaxial force. This unique process offers an inexpensive route to generate various periodic nanostructures rapidly.

Keywords: nanoreplica molding, plasmonic crystal, imprint lithography

1. INTRODUCTION

Because periodic nanostructures, such as 1D and 2D sub-wavelength gratings, are capable of controlling light propagation and enhancing light-matter interactions, they are critical to a broad range of optical applications.[1] For example, they have been exploited in various photonic devices, including diffraction gratings, distributed feedback lasers, grating couplers, wire grid polarizers, and photonic crystals.[2-4] In the past, the need to work on a sub-micrometer scale limited the fabrication of periodic nanostructures. Conventional lithography methods, such as using e-beam and deep ultraviolet, are either too expensive or have insufficient throughput for wafer-scale fabrications. Recently, interference lithography and imprint lithography have been successfully applied to address this issue.[5-9] In particular, soft lithography provides the capability of inexpensive, roll-to-roll manufacture of periodic nanostructures. The soft lithography processes utilize molds with nanoscale features that can be transferred to a polymer material at room temperature, without the need for excessive pressure.[10-12]

One major drawback of the soft lithography is the high cost of molds. In order to introduce or modify a pattern, a brand new mold must be fabricated. To facilitate the production of different patterns, in particular, the periodic structures, a few programmable soft lithography technologies have been demonstrated. For example, Lee *et al.* used the thermal tuning method to program nanoscale patterns carried by a thermoplastic substrate to generate a variety of patterns.[7] In this paper, we present multiple plasmonic crystals fabricated by a programmable nanoreplica molding process. This technique exploits mechanical stretching of an elastic polydimethylsiloxane (PDMS) mold to create periodic structures with various periods. When a force is applied, the surface of the PDMS mold adjusts itself to a negative surface profile of the desired periodic structure. Replicating the stretched feature into a UV-curable polymer (UVCP) yields programmable nanostructures using a process that is inexpensive and amenable to scale-up. Following the replica molding, the produced periodic structures may be coated with a metal or dielectric thin film; some examples are gold, silver, and indium tin oxide, or titanium dioxide. With a 100 nm-thick coating of silver, we demonstrate the fabrication of 2D plasmonic crystals that exhibit surface plasmon resonances (SPRs) spanning the wavelength range of 410 nm to 570 nm.

*menglu@iastate.edu; phone 1 515 294-9951

Advanced Fabrication Technologies for Micro/Nano Optics and Photonics IX, edited by Georg von Freymann, Winston V. Schoenfeld, Raymond C. Rumpf, Proc. of SPIE Vol. 9759, 97591G
 · doi: 10.1117/12.2212053

2. RESULTS AND DISCUSSION

2.1. Programmable nanoreplica molding process

The major steps (mold preparation, mold stretching, pattern transfer, and mold release) involved in the programmable nanoreplica molding process are summarized in Figure 1. As the initial step, a PDMS mold was replicated from a rigid glass stamp bearing a 2D rectangular array of 150 nm diameter nanoposts with the lattice periods of 300 nm. The glass stamp, with a patterned area of 50 mm × 50 mm, was produced by using a glass thermal imprinting process with a vitreous mold formed by carbonization of furan precursor.[13, 14] The glass master stamp was pre-cleaned and treated using an anti-adhesion silane (Repel Silane, GE Healthcare) in order to facilitate the mold separation. Then, the PDMS mold was produced by the thermally curing of a mixture of PDMS elastomer and curing agent (in a volume ratio of 1:10) on the glass master stamp. The thickness of PDMS molds was controlled to be 2 mm. After curing at 100°C for 4 hours, the cured PDMS was separated from the glass master stamp. The PDMS mold was subsequently trimmed into a rectangular shape that has a length and width of 50 mm and 15 mm, respectively.

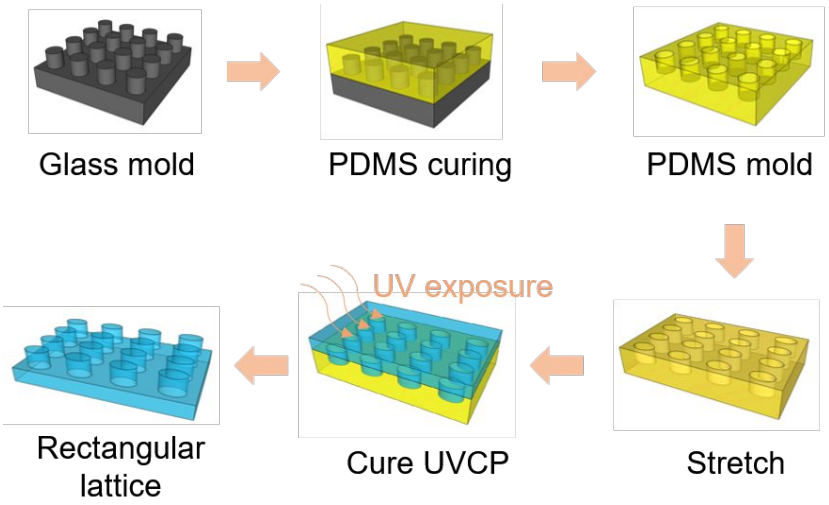

Figure 1. Process flow of the programmable nanoreplica molding for the fabrication of periodic patterns. The PDMS mold is replicated from the glass master stamp. To generate a target pattern, the PDMS mold is carefully pulled. Then, the stretched surface feature is molded in UVCP using the replica molding process.

Next, the PDMS mold was carefully stretched to obtain a particular lattice pattern. The orientation of the lattice on the PDMS mold was identified and marked. To stretch the mold, we placed it between two grips that were separated by a length of 45 mm on a customized translation stage. One of the grips was fixed and the other one was pulled horizontally. The pulling resulted in a uniaxial force applied to the mold in the plane parallel to its surface. The stretch induces an averaged strain value of $\varepsilon_x = \Delta L/L$, where ΔL represents the amount of deformation. The PDMS mold was held at the desired length during the replica molding process. Along the direction of the stretch, the array is elongated and its period increases. On the other hand, the array is compressed in the perpendicular direction of the stretch, and thus, the array period is reduced. A layer of liquid UVCP (NOA 88, Norland Product Inc.) was squeezed between the stretched PDMS mold and a polyethylene terephthalate (PET) substrate. The UV-curing process took place by exposing the PET/liquid UVCP/PDMS stack to UV light for 5 min. After curing, the replica and the PDMS mold were separated by peeling the coverslip away from the PDMS mold. The solidified polymer preferentially bonds to the PET substrate. Following the replica molding, a layer silver thin film was deposited over the surface relief 2D grating by electron-beam evaporation to complete the fabrication of plasmonic crystals.

Figure 2(a) schematically illustrates how the geometry of the periodic nanostructure is tuned to produce different types of arrays. The blue dots represent the nanoposts of the un-stretched square lattice with a period of 300 nm. When a uniaxial force is applied along the horizontal axis, the square lattice is changed to a rectangular one, as shown by the array of cherry-colored dots. Figure 2(b) and 2(c) show the scanning electron microscopy (SEM) images of replicated square and rectangular array, respectively. The rectangular array in Figure 2(d) was fabricated when the PDMS mold

was under a strain of 40%. The period of the array increases to 420 nm along the direction of the applied force. The lattice shows a slight shrinkage in the direction perpendicular to the force, with a period of 258 nm. While the cross section of the nanoposts changes from circular to elliptical, the duty cycles of the periodic structure (post dimension/period) remain unchanged.

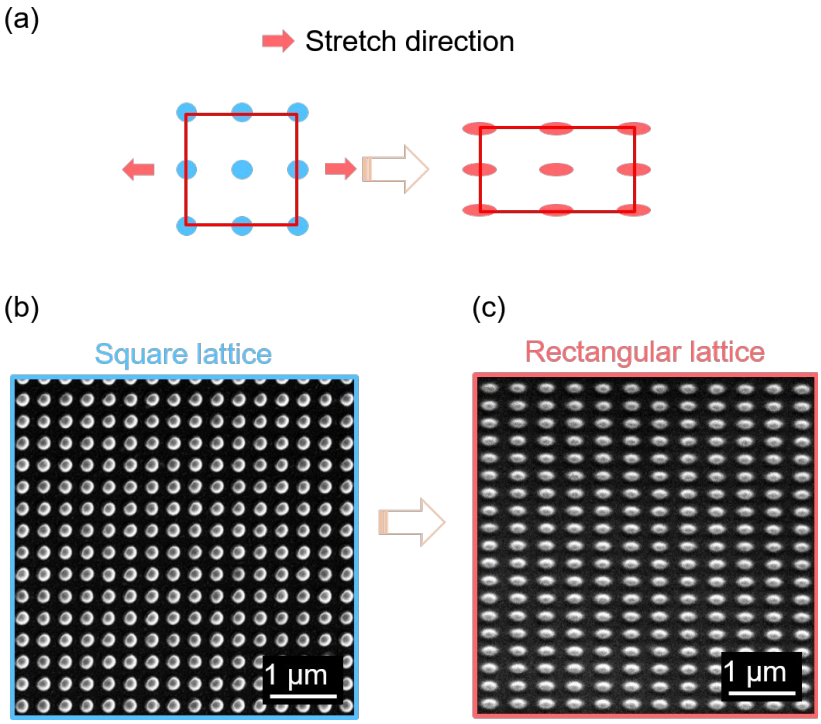

Figure 2. Two different nanopost arrays replicated using a single PDMS mold. (a) Schematics of the mold programming process. (b) and (c) SEM images of nanopost arrays with square lattice and rectangular lattice, respectively.

2.2. Plasmonic crystals

As an example, we applied the process described above to fabricate multiple plasmonic crystals with different periodic arrays. As a result of the different geometries, these arrays exhibit distinct plasmonic resonances. As shown in Figure 3(a), the plasmonic crystal structure consists of a replicated 2D array of nanoposts with a 100 nm-thick silver coating, and supports grating-coupled surface plasmon resonance (SPR) modes, namely the lattice plasmon mode. Excitation light that meets the resonance condition can be coupled into an SPR mode and may be strongly absorbed. As a result, the reflection spectrum exhibits a dip with the minimum reflectance at the SPR wavelength (λ_{SP}). The resonance wavelength can be estimated using the equation: $\lambda_{sp} = \sqrt{\frac{\varepsilon_d \varepsilon_m}{\varepsilon_d + \varepsilon_m}} \cdot \frac{\Lambda}{\sqrt{i^2 + j^2}}$, where Λ is the period of the grating, (i, j) represent the Bragg resonance orders, and ε_m and ε_d are the dielectric constants of metal and surrounding medium, respectively.[15] Because the SPRs of plasmonic crystals are primarily determined by the grating period, the programmable replica molding process can efficiently tune the periodic array to achieve SPR modes at the desired spectral position.

In fact, the resonance wavelength varies proportionally to the strain (ϵ) that is generated in the PDMS mold by the uniaxial stretch. In order to experimentally investigate the correlation between λ_{SP} and ϵ, we replicated 10 different arrays of nanoposts by placing the PDMS mold under a range of strains (ϵ = 0%, 2.5%, 5%, 7.5%, 10%, 15%, 20%, 25%, 30%, and 35%). The replicated 2D gratings were subsequently coated with a 100 nm-thick silver film to form the plasmonic crystals. Reflection spectra of the plasmonic crystals were measured to identify their resonance wavelengths.

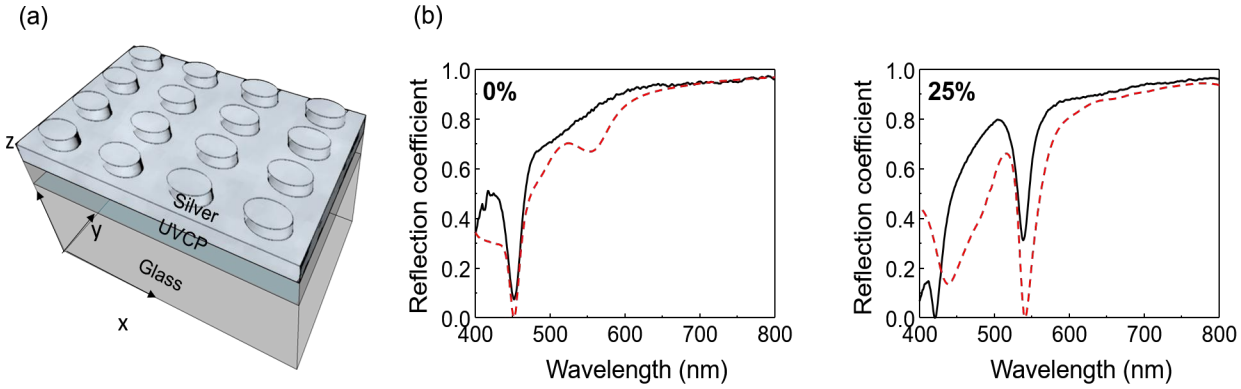

Figure 3. 2D plasmonic crystals with two different lattices. (a) Schematic of a silver-coated plasmonic slab. (b) Simulated and measured reflectance of plasmonic crystals fabricated with PDMS under 0% and 25% strains. The black solid and red dashed curves represent the measurement and the simulation results, respectively.

For purpose of comparison, we have also performed numerical calculations of the spectral responses of the plasmonic devices using the rigorous coupled wave analysis (RCWA). In this work, we utilized a software package (DiffractMod, Rsoft Design Group) to calculate the reflection spectra. The simulation region was setup to the unit volume of the periodic structures. Ten spatial harmonics were used at both *x*- and *y*-directions, defined in Figure 3(a). The devices were illuminated from the direction normal to the surface by a plane wave. The incident wave was linearly polarized with the electric field oriented at 45° to *x*-axis in *x*-*y* plane. The material properties of silver were taken from the Palik's handbook, and then fitted by the multi-coefficient model in the wavelength range from 300 nm to 1000 nm. Reflection spectra of plasmonic crystals were calculated in the wavelength range from 375 nm to 775 nm.

2.3. Optical characterization

Reflection spectra of plasmonic crystals were measured using a white light reflection setup. A halogen lamp was used as a broadband excitation source, and was coupled into a bifurcated fiber (BFY50HS02, Thorlabs), with a fiber tip collimator at the exit. An iris and a linear polarizer were placed in front of the collimator to control the spot size and polarization of the incident beam. The illumination assembly was attached to a kinematic mount for precise adjustment of the angle of incidence. The reflected light was coupled into a spectrometer (USB2000, OceanOptics) through the same bifurcated fiber. For measurement of its reflection spectrum, a plasmonic crystal sample was mounted on a motorized *x*-*y* translation stage and immersed in deionized water. A silver-coated mirror was used as the reference for reflectance. The measured spectra were fitted using a second-order polynomial function to find the resonance wavelength of the plasmonic modes.

Figure 3(b) compares the measured and simulated reflection spectra of devices fabricated with 0% and 25% strain. With 0% strain, the device exhibits a reflection dip at λ_{SP} = 456 nm; the *x*- and *y*-polarized SPR modes coincide in wavelength because the array structure is symmetric. As shown in Figure 4(a), the stretch applied during molding splits the differently polarized resonance modes. The SPR mode with the electric field polarized along the *x*-axis shifts to longer wavelengths with increased stretch; the shift is proportional to the degree of stretching. The corresponding compression along the *y*-axis causes the *y*-polarized SPR mode to move to shorter wavelengths. For ϵ = 35%, the plasmonic resonances are shifted by 111 nm and -41 nm for the *x*- and *y*- polarizations, respectively. Figure 4(b) summarizes λ_{SP} as a function of strain for both polarizations. The measured resonance wavelengths are fitted by straight lines with slopes of λ_{SP}/ϵ = 3.13 and -1.14 nm/(% strain) for the *x*- and *y*-polarizations, respectively.

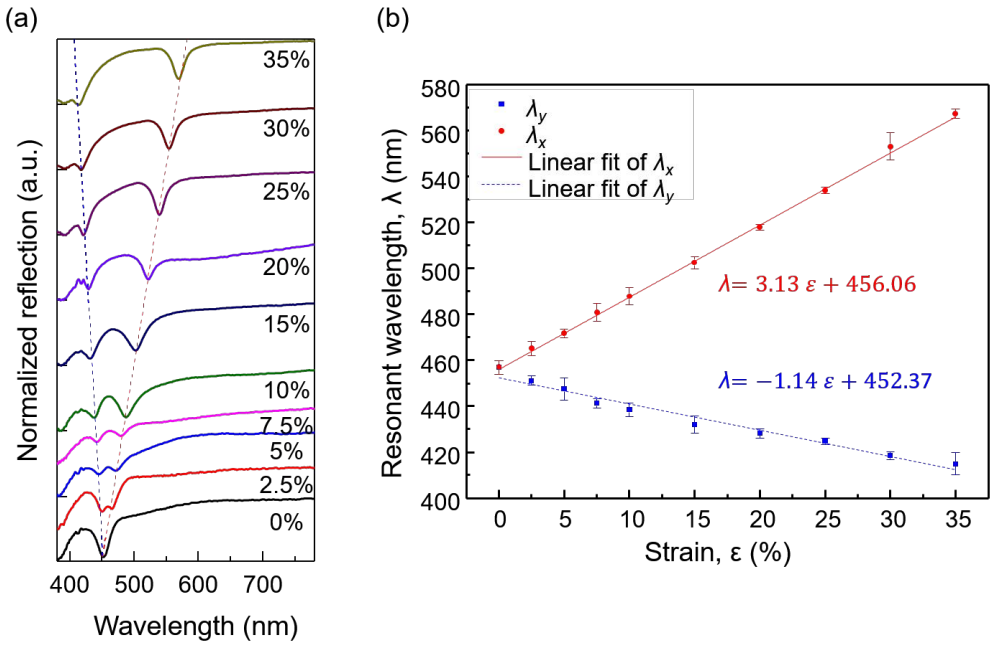

Figure 4. (a) The SPR reflection dips for plasmonic slabs fabricated with 0%, 2.5%, 5%, 7.5%, 10%, 15%, 20%, 25%, 30%, and 35% strain, respectively. The split between the dips for *x*- and *y*-polarized modes follows the lattice period deviations in the *x*-direction (elongation) and *y*-direction (compression). (b) Plasmonic resonance wavelength with respect to applied strain. The SPR dips in the stretched and compressed directions from the experimental data in (a) are shown by the red dots and blue squares, respectively; linear fits to the resonance wavelengths, by the solid red and dashed blue lines. The error bars represent the standard deviation of 10 measurements taken at different locations on the sample.

3. CONCLUSION

In summary, a programmable nanoreplica molding method is developed to facilitate the fabrication of grating-based nanophotonic devices. Using a single PDMS mold, this fabrication method is capable of producing sub-wavelength structures with various lattice geometries. The stretchable PDMS mold, which was replicated from a glass stamp, is exploited to generate periodic nanostructures using UVCP material on flexible PET substrates. During nanoreplica molding, the PDMS mold was stretched precisely to produce the desired lattice geometry. Ten different plasmonic crystals were fabricated and characterized. The optical resonances of these devices were experimentally measured and compared to simulation results. The developed approach can achieve SPR wavelength ranging from 456 nm to 566 nm with the increments of nm/(% strain). Since the PDMS can endure as high as 100%,[16, 17] the increase of the applied stain can further extend the range of the resonance wavelength tuning.

4. ACKNOWLEDGMENTS

The research was supported by the startup fund of Iowa State University and the 3M Non-Tenured Faculty Award.

REFERENCES

[1] Busch, K., Von Freymann, G., Linden, S., Mingaleev, S. F., Tkeshelashvili, L., and Wegener, M., "Periodic nanostructures for photonics," *Phys. Rep.,* 444(3-6), 101-202 (2007).
[2] Collin, S., "Nanostructure arrays in free-space: optical properties and applications," *Rep. Prog. Phys.,* 77(12), (2014).

[3] Johnson, S. G., Fan, S. H., Villeneuve, P. R., Joannopoulos, J. D., and Kolodziejski, L. A., "Guided modes in photonic crystal slabs," *Phys. Rev. B,* 60(8), 5751-5758 (1999).
[4] Taillaert, D., Van Laere, F., Ayre, M., Bogaerts, W., Van Thourhout, D., Bienstman, P., and Baets, R., "Grating couplers for coupling between optical fibers and nanophotonic waveguides," *Jpn. J. Appl. Phys.,* 45(8A), 6071-6077 (2006).
[5] Chou, S. Y., Krauss, P. R., and Renstrom, P. J., "Nanoimprint lithography," *J. Vac. Sci. Technol. B,* 14(6), 4129-4133 (1996).
[6] Zhao, X. M., Xia, Y. N., and Whitesides, G. M., "Soft lithographic methods for nano-fabrication," *J. Mater. Chem.,* 7(7), 1069-1074 (1997).
[7] Lee, M. H., Huntington, M. D., Zhou, W., Yang, J. C., and Odom, T. W., "Programmable Soft Lithography: Solvent-Assisted Nanoscale Embossing," *Nano Lett.,* 11(2), 311-315 (2011).
[8] Pokhriyal, A., Lu, M., Chaudhery, V., Huang, C. S., Schulz, S., and Cunningham, B. T., "Photonic crystal enhanced fluorescence using a quartz substrate to reduce limits of detection," *Opt. Express,* 18(24), 24793-24808 (2010).
[9] Lu, M., Choi, S. S., Irfan, U., and Cunningham, B. T., "Plastic distributed feedback laser biosensor," *Appl. Phys. Lett.,* 93(11), (2008).
[10] Lee, H. S., Kim, D. S., and Kwon, T. H., "UV nano embossing for polymer nano structures with non-transparent mold insert," *Microsyst. Technol.,* 13(5-6), 593-599 (2007).
[11] Kooy, N., Mohamed, K., Pin, L. T., and Guan, O. S., "A review of roll-to-roll nanoimprint lithography," *Nanoscale Res. Lett.,* 9, (2014).
[12] Ahn, S. H., and Guo, L. J., "Large-Area Roll-to-Roll and Roll-to-Plate Nanoimprint Lithography: A Step toward High-Throughput Application of Continuous Nanoimprinting," *Acs Nano,* 3(8), 2304-2310 (2009).
[13] Ju, J., Lim, S., Seok, J., and Kim, S. M., "A Method to Fabricate Low-Cost and Large Area Vitreous Carbon Mold for Glass Molded Microstructures," *Int. J. Precis. Eng. Man.,* 16(2), 287-291 (2015).
[14] Ju, J., Han, Y., Seok, J., and Kim, S. M., "Development of Low-cost and Large-area Nanopatterned Vitreous Carbon Stamp for Glass Nanoreplication," *2012 12th Ieee Conference on Nanotechnology (Ieee-Nano)*, (2012).
[15] Chang, S. H., Gray, S. K., and Schatz, G. C., "Surface plasmon generation and light transmission by isolated nanoholes and arrays of nanoholes in thin metal films," *Opt. Express,* 13(8), 3150-3165 (2005).
[16] Zhao, S., Xia, H., Wu, D., Lv, C., Chen, Q. D., Ariga, K., Liu, L. Q., and Sun, H. B., "Mechanical stretch for tunable wetting from topological PDMS film," *Soft Matter,* 9(16), 4236-4240 (2013).
[17] Lin, P. C., Vajpayee, S., Jagota, A., Hui, C. Y., and Yang, S., "Mechanically tunable dry adhesive from wrinkled elastomers," *Soft Matter,* 4(9), 1830-1835 (2008).